RSC Advances




ROYAL SOCIETY OF CHEMISTRY

www.rsc.org/advances

# Structural modification of Acrylonitrile–Butadiene–Styrene waste as an efficient nanoadsorbent for removal of metal ions from water: Isotherm, kinetic and thermodynamic study

**Arameh Masoumi, Khadijeh Hemati, Mousa Ghaemy***

**Abstract**

Acrylonitrile–butadiene –styrene (ABS) terpolymer waste was recycled via amidoximation of the nitrile groups using hydroxylamine hydrochloride. The resulting modified ABS (AO-ABS) nanoparticles possessing amidoxime functional groups, $–C(NH_2)=NOH$, has been shown to be an effective adsorbent for the removal of heavy metal ions from aqueous solutions. The effect of pH, adsorbent dosage, immersion time, concentration of adsorbate and temperature on the extent of adsorption was investigated to understand adsorption isotherms, kinetics and thermodynamics. The results showed that the interaction between metal ions and $–C(NH_2)=NOH$ groups agree with the Langmuir isotherm and pseudo-second-order kinetic model and the maximum adsorption capacities ($Q_m$) were found in the range of 56.5, 56.0, 53.47, and 51.28 (mg $g^{-1}$) for the adsorption of metal ions $Pb^{2+}$, $Cu^{2+}$, $Cd^{2+}$, $Zn^{2+}$. Thermodynamic studies of metal ions indicated that the adsorption process was spontaneous and endothermic with $\Delta H$ and $\Delta S$ values in the range of 22.2-36.4 kJ $mol^{-1}$ and 74.7-128.6 J $k^{-1}$ $mol^{-1}$, respectively. Not having hydrolysable linkages, desorption process of AO-ABS has been carried out in HCl (0.1 M) without losing much its activity. It can be suggested that amidoximation is a suitable recycling method for new applications of ABS waste and it seems to be applicable in large scale water softening processes.

**Keywords**: recycling, acrylonitrile–butadiene–styrene, amidoximation, metal ions adsorption, isotherm, kinetic

## Introduction

Excellent properties such as high toughness and resistance to heat and chemicals and also intermediate price, make acrylonitrile–butadiene–styrene (ABS) terpolymer as one of the most frequently applied engineering thermoplastic widely used in electric and electronic industry, automobiles, communication instruments, and other commodities.[1–3] Economic growth, especially in the last decades, leaded to large amounts of waste plastics and brought many environmental problems. Through the traditional methods of waste plastics treatment, combustion and burial were limited due to increasing air and water pollutions but recycling by blending or modification techniques has drawn much attention recently and been the subject of many research studies.[4–6] Heavy metal pollution in environmental samples is critical due to their toxic nature, non-biodegradability and non-decomposability. Various methods of heavy metal removal from wastewaters have been reported in the literatures.[7–10] Among these, adsorption via various types of adsorbents is regarded as a facile and effective method for wastewater treatment.[11–14] The adsorption properties depend on the functional group(s) on the surface of adsorbents and it has been reported that nitrogen-based functional groups such as, amino, imidazole, amidoxime, and hydrazine groups was more effective in forming complexation with metal ions compare to other chelating groups.[15–17] Through reliable treatment processes, adsorption of heavy metals from aqueous solutions by modified wastes seems to be a feasible and economical solution.[18–21] As reported in the literatures, among various types of chelating groups, amidoxime groups (-C-($NH_2$)=NOH) have been widely introduced on solid adsorbents because of their strong chelation properties towards metal ions.[22–26] There has been an increasing interest in using polymer wastes as adsorbents for metal ion removal from aqueous solutions. In this study, due to large availability of ABS waste and low recycling modifications,

amidoximated ABS (AO-ABS) was prepared through a simple one-step reaction of ABS with hydroxylamine hydrochloride solution to introduce amidoxime functional groups – $C(NH_2)$=NOH in the polymer. Fourier transform infrared spectroscopy (FT-IR) and atomic force microscopy (AFM) was employed, respectively, to examine the composition and the surface morphology of AO-ABS. A series of batch adsorption experiments was conducted to investigate the adsorption isotherms, kinetics and thermodynamics of the AO-ABS as a nanoadsorbent in removing metal ions such as $Pb^{2+}$, $Cu^{2+}$, $Zn^{2+}$, $Cd^{2+}$ from aqueous solutions. Therefore, the effect of various factors, such as immersion time, pH of the solution, amount of adsorbent, initial metal ion concentration and temperature were investigated. The experimental data were fitted to Freundlich and Langmuir adsorption isotherm models. The results were also analyzed on the basis of Lagergren pseudo-first order and pseudo-second order kinetic equations. The reversibility of metal sorption by applying 0.1 M HCl was also explored to evaluate reusability of the adsorbent.

## Materials and Methods

### Chemicals and reagents

Acrylonitrile–butadiene–styrene (ABS) terpolymer wastes without having metal parts were provided from a local electrical/electronics industry (primarily in white goods). Hydroxylamine hydrochloride ($NH_2OH{\cdot}HCl$) and sodium dodecyl sulfate (SDS) were purchased from Fluka (Darmstadt, Germany) and used without further purification. Stock solutions of metal ions were prepared from $Pb(NO_3)_2$, $CuCl_2{\cdot}2H_2O$ salts and $Zn(NO_3)_2{\cdot}4H_2O$ and $Cd(NO_3)_2{\cdot}4H_2O$ (1000 mg L−1) standard solutions. Distilled water (<1microsiemens [μS]) was used for dilution of the stock solutions. The alkali used was sodium hydroxide (NaOH) and the acids used were hydrochloric acid (HCl) and nitric acid ($HNO_3$), all in laboratory grade.

### Methods of characterization

FT-IR analysis was carried out on a Bruker Tensor 27 spectrometer (Bruker, karlsrohe, Germany). Samples were prepared by dispersing in dry KBr pellets and recorded between 4000 and 400 $cm^{-1}$. Atomic force microscopic (AFM) Easy Scan 2 Flex AFM (Swiss Co.) was also used to investigate the surface phase and topography of the sample before and after the sorption process. A PHS-3C pH-meter (Shanghai, Tianyou) was used for pH measurements. The concentration of metal ions in the solution was measured by use of a flame atomic absorption instrument (Hewlett- Packard 3510) (AAS).

**Preparation of amidoximated acrylonitrile–butadiene–styrene (AO-ABS)**

ABS waste particles was first washed with hot water to remove the dust, and purified with hot ethanol extraction to remove the grease and then dried under vacuum for 48 h. The dried ABS particles were grinded into powder using an abrasive. In order to remove the additives, the ABS powder was dissolved in dichloromethane by stirring at room temperature for 24 h. The solution was filtered to remove the possible insoluble parts, and then was poured into methanol to precipitate. The precipitated powder was filtered, washed several times with methanol and dried in the vacuum oven at 80 °C for 8 h.

In order to obtain amidoxime-functionalized ABS (AO-ABS), the conversion of nitrile groups of ABS powder to amidoxime groups was carried out using hydroxylamine hydrochloride in aqueous solution, following procedure in the previous paper.[27] 1 g ABS purified powder was dispersed in 30 mL distilled water in a beaker and sonicated for 60 minutes. This ABS suspension solution was added into a 250 mL three-necked flask equipped with a condenser and a magnet stirrer containing 0.5 g sodium dodecyl sulfate (SDS) dissolved in 30 mL distilled water. 6.94 g $NH_2OH{\cdot}HCl$ and 4 g NaOH (1:1, mole ratio) were dissolved in 50 mL distilled water with stirring to neutralize HCl (pH 6.5) and then was added to the mixture of ABS/SDS solution in the flask. The mixture was refluxed under $N_2$ atmosphere for 4 h. The suspension

solution was filtered and the obtained solid product was washed several times with distilled water to remove the remaining salts and dried in a vacuum oven at 60 ºC.

**Adsorption experiments**

Batch experiments were conducted to study the metal ions adsorption behavior of ABS and AO-ABS powder in aqueous media. The sorption equilibrium experiments include the effect of pH values (2.0 – 8.0), amount of adsorbent (25-200 mg), initial metal ion concentration (20–300 mg $L^{-1}$), immersion time (30-240 min) and temperature (293-333K) on sorption, determination of the maximum binding capacity, isotherm, kinetic and thermodynamic of adsorption, respectively. The effect of each factor was conducted at constant conditions of 0.1 g adsorbent powder dispersed in 25 mL of each metal ion solution (100 mg $L^{-1}$) for 120 min with stirring at 300 rpm and 303 K, varying the initial level of related factor. After the equilibrium in all experiments, the two phases were separated and the concentration of metal ion was analyzed by using AAS. The instrument responses were periodically checked with known heavy metal standard solutions. The experiments and analyzes were performed in replicates of three. The following equations were used for calculating the percentage removal of heavy metal ions (%R) and the adsorption capacity ($Q_e$) that represents the amount of adsorbed ions (mg $g^{-1}$), respectively.

$$R(\%) = (\frac{C_0 - C_e}{C_0}) \times 100 \quad (1)$$

$$Q_e = (\frac{C_0 - C_e}{W}) \times V \quad (2)$$

where $C_0$ and $C_e$ are the concentrations of metal ions in the initial solution and in the aqueous phase after adsorption, respectively (mg $L^{-1}$), V is the volume of the aqueous phase (L) and W is the weight of the polymer (g).

**Metal adsorption/desorption experiments**

To assess the reusability of the adsorbent, adsorption/desorption cycles were conducted as follows: each adsorption experiment consisted of 0.5 g AO-ABS sample powder loaded with metal ion from aqueous solution with initial concentration $C_0$= 100 mg $L^{-1}$. After the adsorption experiments, metal ion-loaded AO-ABS powder in the flask were collected by filtration, washed with deionized water and stirred at 200 rpm in 50 mL solution of 0.1 M HCl at 50 °C for 12 h to desorb the metal ions. The regenerated adsorbent was then filtered and separated from solution, neutralized with NaOH, washed with deionized water and subjected to chelation process again, and this cycle was repeated 3 times. All the initial and final metal ions concentrations in the solution samples were determined by atomic absorption spectrophotometer.

The desorption ratio (D) was calculated using the following equation;

$$D(\%) = \frac{A}{B} \times 100 \quad (3)$$

where A is the amount of metal ions desorbed to the elution medium (mg) and B is the amount of metal ions adsorbed on the adsorbent (mg).

## Results and discussion

### Fabrication and characterization of AO-ABS adsorbent

**Fig. 1** illustrates the single-step reaction of hydroxylamine hydrochloride with nitrile groups of ABS. The nitrile groups on the side chains of ABS react with $H_2NOH.HCl$ in sodium hydroxide solution and convert to amidoxime functional groups through nucleophilic addition. In this study, FT-IR analysis was used to identify the presence of certain functional groups on a solid surface in material modification because each specific chemical bond often shows a unique energy absorption band. **Fig. 2** (a-c) shows FT-IR spectra of ABS, AO-ABS and metal-adsorbed AO-ABS. The characteristic absorption bands for the ABS in **Fig. 2a** can be assigned as follows: 3060-2850 $cm^{-1}$(C-H stretching of CH, $CH_2$ and aromatic ring), 2238 $cm^{-1}$ (C≡N stretching),

1602 $cm^{-1}$(cis-1,4-C=C stretching), 1450-1500 $cm^{-1}$ (C-H bending of aromatic ring), 966 $cm^{-1}$ (trans-1,4-C=C stretching), 760 and 700 $cm^{-1}$ (Mono-sub phenyl group). After reaction of the ABS with $H_2NOH.HCl$ solution, the spectrum of AO-ABS in **Fig. 2b** shows many significant changes. The characteristic absorption band of C≡N group at 2238 $cm^{-1}$ disappeared completely and new bands were observed at: 1623 $cm^{-1}$, 1586 $cm^{-1}$ and 1219 $cm^{-1}$ corresponding to the stretching vibrations of C=N, N-H and C-N bonds in $–C(NH_2)=NOH$ group, respectively. Also, the weak band with the peak at 3420 $cm^{-1}$ for the ABS was replaced by a strong band with the peak at 3419 $cm^{-1}$ for the AO-ABS which corresponds to the combination of the stretching vibration bands of both OH and $NH_2$ groups. The $NH_2$ and OH groups may be introduced in the polymer structure by a reaction of hydroxylamine hydrochloride with the nitrile group on the ABS. Also there is a change in the absorption bands at 760 and 700 $cm^{-1}$ of ABS after amidoximation where only one sharp absorption band appeared at 760 $cm^{-1}$. This can be due to substitution of aromatic ring with $H_2N^+$ ion at the para position. These observations clearly indicate that amidoxime groups and substituted benzene rings with the amine groups were formed effectively via hydroxylamine treatment, and the corresponding molecular structure change during the preparation of AO-ABS may be proposed as in **Fig. 1**. As can be seen in this figure, amidoxime groups as bidentate ligands are expected to enhance chelating adsorption ability for heavy metal removal. In the FT-IR spectrum of the AO-ABS after metal ion adsorption in **Fig.2c**, there is small shift towards higher frequency which can be taken as evidence for formation of coordination bond between metal ions and functional groups of AO-ABS. 3D AFM micrographs were also used to observe morphological properties of the surface of AO-ABS powder before and after metal ion adsorption. As can be seen in **Fig. 3**, the surface of AO-ABS powder after metal ion adsorption is fully covered with bumps revealing layer of the

absorbed metal ions. The appearance of these bumps (with height of 34 nm in comparison with 23 nm before adsorption) can be due to chelation of metal ions with the functional groups of modified polymer matrix. The SEM images of AO-ABS before and after metal ion adsorption are shown in Fig. 3(c) and (d), respectively. In comparison with SEM images of untreated ABS reported in the previous literatures[4, 6], surface modification through introduction of amidoxime functional groups on the surface of ABS led to the roughness of AO-ABS surface which can be considered as a factor of the increase of metal ion adsorption. As can be seen in Fig. 3, the increase in the average size of the particles from about 234 nm to 539 nm indicates complexation of metal ions with the active sites of polymer.

**Effects of main factors on the adsorption behavior of the AO-ABS**

**Effect of solution pH**

The solution pH is a significant parameter in the adsorption process due to protonation and deprotonation of the acidic and basic groups of the metal complexion ligand which can influence the adsorption behavior for metal ions. To avoid chemical precipitation, adsorption experiments were performed in the pH range of 2.0-8.0. The effect of the initial pH values on the adsorption of tested metal ions is shown in **Fig. 4**(a). The adsorption of all tested metal ions was low at pH 2.0 which can be due to the competitive adsorption between metal ions and available $H^+$ for protonation of the active sites of the adsorbent. It is also possible that at pH 2, the strong electrical repulsion prevented the metal ions from contacting the surfaces of the AO-ABS, resulting in less adsorption of metal ions on the AO-ABS. All metal ions displayed a general trend of increased adsorption on the AO-ABS with the increase of solution pH values from 2.0 to 8.0. With the increase of pH, the electrical repulsion force become weaker and the metal ions may be transported to the surface of the AO-ABS, and become attached on the surface due to the action of other factors such as Van der Waals force, the formation of chemical and nonchemical

bonds, and so forth. Particularly, the presence of $NH_2$, NOH, and OH groups on the surface of the AO-ABS, may result in the formation of metal complexes through chelating or metal exchanges. At pH 6.0, the removal efficiency (%R) for $Pb^{2+}$, $Cu^{2+}$, $Zn^{2+}$, $Cd^{2+}$ were 90.8%, 89.6%, 84.5%, and 82.0%, respectively, and the adsorption capacities were in the range of 20.5-22.70 mg $g^{-1}$.

**Effect of adsorbent dosage**

The removal efficiency (%R) of metal ions as a function of the adsorbent dosage was investigated and the results are shown in **Fig. 4**(b). As can be seen, the adsorption of the tested metal ions increased with increasing the amount of AO-ABS. This increase can be due to presence of more binding sites on the surface of adsorbent to form complexes with metal ions. However, the maximum adsorption occurred for 100 mg of adsorbent where further increase in adsorbent dosage had less effect on metal removal. The adsorption efficiency at the equilibrium was in the range of 82-90% for $Cd^{2+}$, $Zn^{2+}$, $Cu^{2+}$, $Pb^{2+}$ ions. However, the metal ion adsorption did not increase with further increase of the adsorbent which can be due to the exhaustion of the active functional groups in the AO-ABS.

**Effect of initial metal ion concentration (Isothermal adsorption studies)**

The rate of adsorption is an important parameter for efficient adsorption and depends on the initial concentration of metal ions. The percentage removal of the tested metal ions at different metal ion concentration (20 to 300 mg $L^{-1}$), keeping all other parameters constant and using AO-ABS sorbent at 303 K, is presented in **Fig. 4**(c). As the initial metal ions concentrations increased, the removal percentage decreased about 30% for each metal ion, while it is clear from **Fig. 5** that the sorption amount or adsorption capacity of metal ions increased with increase in the initial ion concentration. The adsorption isotherms describe the effect of different initial concentrations of metal ion on the adsorption capacity of the adsorbent, leading to finding the

best equilibrium position in the adsorption process. Among different equilibrium isotherm equations the Freundlich and Langmuir models are the most widely used to evaluate the surface properties of an adsorbent.[28,29] The Freundlich model (Eq. 4) assumes that adsorption occurs on heterogeneous surfaces and there is interaction between the adsorbed molecules, while the Langmuir isotherm model (Eq. 5) is often used to describe the equilibrium adsorption isotherms of homogeneous surfaces.[30, 31]

$$\ln Q_e = \ln K_f + \frac{1}{n} \ln C_e \quad (4)$$

$$\frac{C_e}{Q_e} = \frac{1}{Q_m K_L} + \frac{C_e}{Q_m} \quad (5)$$

where $Q_e$ and $C_e$ are the equilibrium adsorption capacity (mg $g^{-1}$) and the equilibrium concentration (mg $L^{-1}$), respectively. $Q_m$ is the maximum metal ion uptake capacity (mg $g^{-1}$). $K_f$ and $K_L$ are model constants related to the adsorption capacity and adsorption energy (L $mg^{-1}$) and were predicted from the plot between *ln* $Q_e$ and *ln* $C_e$ and between $\frac{C_e}{Q_e}$ and $C_e$, respectively. From the experimental results presented in Table 1, $Q_m$ values were found as 56.5, 56.0, 53.47, and 51.0 (mg $g^{-1}$) for adsorption of $Pb^{2+}$, $Cu^{2+}$, $Cd^{2+}$, and $Zn^{2+}$. The maximum adsorption capacities of the tested metal ions were almost close, and the high value for $Pb^{2+}$ can be due to formation of metal complexes with both the nitrogen atoms in the amine groups and the oxygen atoms in the hydroxyl groups.[32] The values of the correlation coefficients obtained from the linear forms of the Langmuir and Freundlich equations and the results were shown in supporting information in **Fig. 1S** and **2S**, respectively. According to correlation coefficient ($R^2$) values which were tabulated in **Table 1**, the Langmuir isotherm equation has better conformity with the experimental data than Frendlich model which assumes that all sites possess equal affinity for the

adsorbate.[33] The $Q_m$ values of AO-ABS obtained by the Langmuir equation are compared with other adsorbents found from literatures and summarized in **Table 2**. According to this table, the adsorption capacity of AO-ABS adsorbent is close to or much higher than the reported adsorbents. This indicates that amidoximated ABS can be a good candidate for the applications related to heavy metal ion removal.

**Effect of immersion time (adsorption kinetics studies)**

Immersion time and rapid sorption are the significant parameters of an adsorbent for successful practical applications. The rate of removal process was investigated by increasing the immersion time on metal ions adsorption in the range of 30-240 min, while keeping all other parameters constant. **Fig. 4**(d) shows the typical results of time-dependent adsorption performances of AO-ABS in removing metal ions from aqueous solutions. With increasing immersion time, the amount of adsorption for all tested metal ions on the AO-ABS increased rapidly in the first 60 min and then augmented slowly and approached the adsorption equilibrium in about 120 min, as shown in **Fig. 4**(d). In general, this type of adsorption behavior is typical of the specific adsorption process in which adsorption rate is dependent upon the number of available adsorption sites on the surface of the adsorbent and the amount of adsorption is usually controlled by the attachment of metal ions on the surface. Therefore, the initial fast adsorption is due to high concentration of metal ions and also number of free adsorptive sites, which slowed down at a later stage and reached an equilibrium level because of decrease in metal ion concentration and also exhaustion of free adsorptive sites. In this case, the AO-ABS had a significantly higher adsorption capacity for tested metal ions than ABS, confirming that introduction of bi-dentate amidoxime functional groups on the AO-ABS indeed enhanced the adsorption of metal ions. In view of the fact that the total surface area (or weight) of the AO-

ABS and ABS used in the experiments was the same but the amount of metal ions adsorbed on the ABS was considerably lower than that of the AO-ABS, it can be concluded that there were more adsorption sites on the AO-ABS than on the ABS and the adsorption was attachment-controlled because the transport of metal ions from the bulk solution to the surface of the adsorbent was essentially the same in the experiments. According to the results, the adsorption capacity ($Q_e$) reached the equilibrium values of 22.5, 22.4, 21.0 and 20.5 mg $g^{-1}$ for $Pb^{2+}$, $Cu^{2+}$, $Zn^{2+}$ and $Cd^{2+}$, respectively. Because the equilibrium concentration was not seriously influenced by increased retention time, the optimum immersion time was considered to be 120 min for other experiments. At the optimum conditions, the above values of $Q_e$ could be compared to the removal percentages (90.8%, 89.6%, 84.5%, and 82.0% for $Pb^{2+}$, $Cu^{2+}$, $Zn^{2+}$ and $Cd^{2+}$, respectively). To clarify the adsorption mechanism of metal ions on AO-ABS, the experimental data were tested using pseudo-first-order (the most reliable kinetics equation suitable only for the rapid initial phase, Eq. 6) and pseudo-second-order (for predicting the kinetic behavior of metal ion adsorption with chemical sorption as a rate controlling step, Eq. 7) kinetic equations as follows:

$$\log(Q_e - Q_t) = \log Q_e - \frac{K_L}{2.303} t \quad (6)$$

$$\frac{t}{Q_t} = \frac{1}{K_F Q_e^2} + \frac{1}{Q_e} t \quad (7)$$

where $Q_t$ and $Q_e$ (mg $g^{-1}$) are the adsorption capacities at time $t$ and equilibrium, respectively, $k_L$ ($min^{-1}$) and $k_F$ (g $mg^{-1} min^{-1}$) are the equations rate constants and determined via the slopes and intercepts of the linear plots of log ($Q_e - Q_t$) versus $t$ (Eq. 6), and $t/Q_t$ versus $t$ (Eq. 7). To identify the conformity of the models with the experimental data, parameters of the kinetic models and coefficients of determination ($R^2$) were calculated and the results are presented in

**Table 3**. **Fig. 6** shows the linear plots of the kinetic models for all the tested metal ions. Based on the coefficient values shown in **Table 3**, the pseudo-second-order model had the higher conformity with the experimental data. This indicates that the rate-limiting step may be chemisorption process through exchanging of electrons between adsorbent and adsorbate.[40] The adsorption capacities of the tested metal ions on the untreated ABS was also carried out using similar experimental conditions (100 mg adsorbent, 100 mg $L^{-1}$ initial metal ion concentration, pH 6.0, and 120 min) and the results are shown in **Fig. 7**. The adsorption capacities of the tested metal ions on the untreated ABS were in the range of 6.41-8.46 mg $g^{-1}$, comparing with the results obtained on AO-ABS which were in the range of 20.52-22.70 mg $g^{-1}$. These results confirm that structural modification of ABS waste through amidoxime functionalization using one-step reaction, as shown in the FT-IR spectrum in **Figure 2**, can have positive effect on the adsorption ability of ABS for the removal of heavy metal ions from aqueous solutions.

**Adsorption thermodynamic**

The effect of temperature on the sorption of metal ions by AO-ABS was also studied and the results are tabulated in Table 4. The values of thermodynamic parameters ($\Delta H$, $\Delta S$ and $\Delta G$) were calculated using the following classical equations (Eqs. 8-10).[40]

$$\ln k_d = \frac{\Delta S}{R} - \frac{\Delta H}{RT} \quad (8)$$

$$\Delta G = \Delta H - T\Delta S \quad (9)$$

$$\Delta G = -RT \ln k_d \quad (10)$$

where $K_d$ is the pseudo-second-order rate constant, R is the universal gas constant (8.314 J/mol K) and $T$ is the absolute temperature (K). According to Eq. (8), the enthalpy ($\Delta H$) and entropy ($\Delta S$) changes of adsorption can be individually calculated from the slope and intercept of the plot of $ln\ k_d$ versus $1/T$ (**Fig. 8**). The thermodynamic parameters for the adsorption of the tested metal

ions onto AO-ABS powder in aqueous solutions at various temperatures are summarized in **Table 4**. The positive value of $\Delta H$ indicated that adsorption is a chemical endothermic process. The negative $\Delta G$ values in each individual temperature indicated that thermodynamically adsorption is feasible and spontaneous. The increase in the negative value of $\Delta G$ suggests that spontaneous nature of adsorption increases with increasing temperature of adsorption solution. The positive value of $\Delta S$ reveals the increased randomness at the solid–solution interface during the fixation of ion on adsorbent surface.

**Desorption studies**

After the process of adsorption, it is vital to be able to recover the metal ions from adsorbing agent and regenerate and restore the used adsorbent. Since the metal complexes are dissociated in acidic conditions, in which protons compete with the metal ions for donating nitrogen atoms, batch desorption experiments were conducted in the selected acidic conditions (HCl, 0.1 M) and desorption efficiencies were subsequently compared. To determine the reusability of the AO-ABS, consecutive adsorption–desorption cycles were repeated three times under the same conditions. The data were calculated using Eq. 3 without taking into account the unremoved metal ion from the previous desorption cycle, and the results are presented in **Fig. 9**. The adsorption/desorption percentages for $Pb^{2+}$, $Cu^{2+}$, $Zn^{2+}$, $Cd^{2+}$ were 90.8/90, 89.6/86, 84.5/83, and 82/78 %, respectively, after first cycle. Therefore, the unremoved metal ions were in the range of 0.8-4% after first desorption process. The unremoved metal ion in each step has not been taken into account in the calculation of the next adsorption/desorption cycle. As it can be inferred from Figure 9, the removal efficiency of the tested metal ions was affected marginally after three cycles. The desorption percentage of the tested metal ions decreased to about 83, 73, 72 and 68

% for $Pb^{2+}$, $Cu^{2+}$, $Zn^{2+}$ and $Cd^{2+}$, respectively, after three cycles. These results indicate that AO-ABS is suitable for the enhanced removal of the heavy metal ions from aqueous solution.

**Conclusions**

Structural modification can be a way to enhance the adsorption capability of many types of polymers for metal ions. In particular, introducing the amino-hydroxyl groups on an adsorbent is desirable due to the nitrogen and oxygen atoms acting as good chelating agents for the removal of heavy metal ions from aqueous solutions. In this study, amidoximated ABS (AO-ABS) was successfully prepared through a simple one-step and environmental safe reaction of the ABS waste with hydroxylamine hydrochloride. It was found that amino-hydroxyl groups were introduced at the carbons in the nitrile groups (-C≡N). Experimental studies of the removal of heavy metal ions showed that AO-ABS had significantly higher adsorption capacities for metal ions than the untreated ABS. In the solution pH values ranging from 2.0 to 8.0 studied, adsorption amounts for all tested metal ions were generally increased with increasing pH and reached the equilibrium state at pH 6.0. The results showed that the highest removal of the tested metal ions occurs in approximately 120 min at pH 6 for 100 mg of adsorbent and for 100 mg $L^{-1}$ initial metal ion concentration. The maximum adsorption capacities ($Q_m$) were found to be 56.5, 56.0, 53.5 and 51.0 (mg $g^{-1}$) for $Pb^{2+}$, $Cu^{2+}$, $Cd^{2+}$, and $Zn^{2+}$, respectively. The adsorption rates followed the pseudo-second-order rate indicating a chemical adsorption process, and sorption of metal ions on the AO-ABS agreed well with the Langmuir adsorption model. Thermodynamic study showed that $pb^{2+}$ adsorption on the AO-ABS is a favorable chemical process with negative $\Delta G$ and positive $\Delta H$ values. Desorption was performed using 0.1 M HCl and the regenerated adsorbent could be reused with little loss of adsorption capacity. These features show that

amidoximated ABS is an economical and effective way of recycling which can be used for the removal of the heavy metal ions from water and wastewater.

**Notes and References**

Polymer Chemistry Research Laboratory, Chemistry Faculty, University of Mazandaran, Babolsar, Iran.

* Corresponding author. Tel.: +98-11-35342353; FAX: +98-11-35342350 . E-mail address: ghaemy@umz.ac.ir (Mousa Ghaemy).

[1] T. Boronat, V. J. Segui, M. A. Peydro, M. J. Reig, J. Mater. Process. Tech., 2009, 209, 2735–2745.

[2] A. Boldiz and K. Möller, Polym. Degrad. Stabil.,2003, 81, 359–366.

[3] L. B. Brennan, D. H. Isaac, and J. C. Arnold, J. Appl. Polym. Sci., 2002, **86**, 572–578.

[4] S. Lashgari, A. A. Azar, S. Lashgari, and S. M. Gezaz, *J. Vinyl. Addict. Technol*., 2010, **16**, 246–253.

[5] J. L. Vilas and J. M. L. S. Arna, *J. Polym. Environ*., 2010**, 18**,. 71–78.

[6] R. Balart, D. Garcı, M. D. Salvador, and J. Lo, *Eur. Poly. Journal*., 2005, **41**, 2150–2160.

[7] K. Vaaramaa and J. Lehto, *Desalination*., 2003, **155**, 157–170.

[8] B. A. M. Al-rashdi, D. J. Johnson, and N. Hilal, *Desalination.*, 2013, **315**, 2–17.

[9] F. Fu and Q. Wang, *J. Environ. Manage.*, 2011, **92**, 407–418.

[10] H. Ozaki, K. Sharmab, and W. Saktaywirf, *Desalination*., 2002, **144**, 287–294.

[11] A. Murugesan, L. Ravikumar, V. Sathyaselvabala, P. Senthilkumar, T. Vidhyadevi, S. D. Kirupha, S. S. Kalaivani, S. Krithiga, and S. Sivanesan, *Desalination*., 2011, **271**, 199–208.

[12] A. Masoumi and M. Ghaemy, *Express .Polym. Lett.*, 2014, **8**, 187–196.

[13] A. Chen, S. Liu, C. Chen, and C. Chen, *J. Hazard. Mater.*, 2008, **154**, 184–191.

[14] A. Masoumi, M. Ghaemy, and A. N. Bakht, *Ind. Eng. Chem.*, 2014, **53**, 8188–8197.

[15] M. Haratake and K. Yasumoto, *Anal. Chim. Acta*., 2006**, 561**, 183–190.

[16] F. Ge, M. M. Li, H. Ye, and B. X. Zhao, *J. Hazard. Mater*., 2012, **211-212**, 366-372.

[17] A. Kara, L. Uzun, N. Be, and A. Denizli, *J. Hazard. Mater*., 2004, **106**, 93–99.

[18] M. Monier, D. M. Ayad, and A. A. Sarhan, *J. Hazard. Mater.*, 2010**, 176**, 348–355.

[19] A. Dada, A. Olalekan, A. Olatunya, and O.Dada, *J. Appl.Chem*., 2012**, 3**, 38–45.

[20] M. H. Jr, A. A. Abia, and A. I. Spiff, *Bioresource. Technol.,* 2006, ***9****7*, 283–291.

[21] Q. Li, J. Zhai, W. Zhang, M. Wang, and J. Zhou, *J. Hazard. Mater* ., 2007, **141**, 163–167.

[22] T. S. Anirudhan and M. Ramachandran, *Ind. Eng. Chem. Res*., 2008**, 47**, 6175–6184.

[23] B. Gao, Y. Gao, and Y. Li, *Chem. Eng. J*., 2010, **158**, 542–549.

[24] N. Horzum, T. Shahwan, O. Parlak, and M. M. Demir, *Chem. Eng. J*., 2012**, 213**, 41–49.

[25] A. K. Pınar and G. Olgun, ", *J. Appl. Polym. Sci***.,** 2004**, 93**, 1705–1710.

[26] N. Pekel and O. Guven, *React.Funct.Polym.*, 1999**, 39**, 139–146.

[27] A. Masoumi and M. Ghaemy, *Carbohydr. polym*., 2014, **108**, 206–215.

[28] W. Shen, S. Chen, S. Shi, X. Li, X. Zhang, W. Hu, and H. Wang, *J.Member.Sci.*, 2009, **75**, 110–114.

[29] S. Huang and D. Chen, *J. Hazard.Mater*., 2009**, 163**, 174–179.

[30] E. Guibal, M. V. Vooren, B. A. Dempsey, and J. Roussy, *J.Sep.Technol.*, 2006, **41**, 37–41.

[31] S. Deng, G. Yu, S. Xie, Q. Yu, J. Huang, and Y. Kuwaki, *Langmuir*., **24**, 2008, 10961–10967.

[32] S. Deng, R. Bai, J. P . Chen, *Langmuir.,* 2003, **19**,5058-5064.

[33] K. Y. Foo and B. H. Hameed, *Chem. Eng. J.*, 2010, **156**, 2–10.

[34] Li K, Wang X, *Bioresour Technol*., 2009, **100**, 2810-2815.

[35] M. Jr. Horsfall ., A. A. Abia, and A. I. Spiff,. *Bioresource. Technol.,* 2006*, **97***, 283–291.

[36] Z. Reddad, C. Gerente, Y. Andres, and P. Le Cloirec. *Environ. Sci. Technol*., 2002, **36**, 2067–2073.

[37] B. Nasernejad, T. Esslam. Zadeh, B. Bonakdar. Pour, M. Esmaail Bygi, and A. Zamani, *Process. Biochem*., 2005, **40**, 1319–1322.

[38] Q. Li, J. Zhai, W. Zhang, M. Wang, and J. Zhou, *J. Hazard. Mater*., 2006 ,**141**, 163–167.

[39] A. H. Chen, S. C. Liu, and C. Y. Chen, *J. Hazard. Mater*., 2008, **154**, 184–191.

[40] S. Hasan, A. Krishnaiah, T. K. Ghosh, D. S. Viswanath, V. M. Boddu and E. D. Smith, *Ind Eng Chem Res*, 2006, **45**, 5066-5077.

**Captions:**

**Table 1.** The isotherm model constants and correlation coefficients at 303 K and at pH 6.0.

**Table 2.** Comparison of the maximum adsorption capacity of various adsorbents.

**Table 3.** Kinetic models and their statistical parameters at 303 K and at pH 6.0.

**Table 4.** Thermodynamics parameters for adsorption of the tested metal ions on AO-ABS.

**Figure 1.** Conversion of ABS to AO-ABS; mixture of purified ABS waste powder, $NH_2OH.HCL/NaOH$, and SDS in distilled water was refluxed 4 h under $N_2$ atmosphere.

**Figure 2.** FT-IR spectra of ABS (a), AO-ABS (b), and metal-loaded AO-ABS (c)

**Figure 3.** AFM images of AO-ABS before (a) and after (b) $Pb^{2+}$ ion adsorption, and SEM images of AO-ABS before (c) and after (d) $Pb^{2+}$ ion adsorption (Temperature = 303 K, $C_0$ = 100 mg $L^{-1}$, adsorbent dosage = 100 mg/25 mL, pH 6.0, immersion time = 120 min)

**Figure 4.** The effect of solution pH (2.0-8.0) (a), adsorbent dosage (25-200 mg/25 mL) (b), initial metal ion concentration (C0 = 20-300 mg $L^{-1}$) (c) and immersion time (30-240 min) (d) on the removal efficiency of the tested metal ions. (Constant conditions: Temperature = 303 K, C0 = 100 mg $L^{-1}$, adsorbent dosage = 100 mg/25 mL, pH 6.0, immersion time = 120 min, with varying the initial level of related factor).

**Figure 5.** The adsorption isotherms of the tested metal ions on AO-ABS. ($C_0$= 20-300 mg $L^{-1}$, adsorbent dosage = 100 mg/25 mL, pH 6.0, temperature = 303 K, immersion time = 120 min).

**Figure 6.** Kinetic models for the adsorption of the tested metal ions: (a) pseudo-first-order, (b) pseudo-second-order. (Temperature = 303 K, $C_0$ = 100 mg $L^{-1}$, adsorbent dosage = 100 mg/25 mL, pH 6.0, immersion time = 30-240 min).

**Figure 7.** Comparison of the equilibrium adsorption capacity ($Q_e$) of the tested metal ions on the untreated ABS and AO-ABS; (Temperature = 303 K, $C_0$ = 100 mg $L^{-1}$, adsorbent dosage = 100 mg/25 mL, pH 6.0, immersion time = 120 min).

**Figure 8**. Van't Hoff plots of the tested metal ions adsorption (Temperature = 293-333 K, $C_0$ = 100 mg $L^{-1}$, adsorbent dosage = 100 mg /25 mL, pH 6.0, immersion time = 120 min).

Figure 9. Adsorption/desorption percentages of the tested metal ions during 3 cycles. Desorption was carried out in 25 mL solution of HCl (0.1 M) and stirred for 1 h at 303 K.

**Table 1.** The isotherm model constants and correlation coefficients at 303 K and at pH 6.0.

| **Isotherm model** | **Parameters** | ***Pb*$^{2+}$** | ***Cu*$^{2+}$** | ***Zn*$^{2+}$** | ***Cd*$^{2+}$** |
|---|---|---|---|---|---|
| Langmuir | $Q_m$ (mg $g^{-1}$) | 56.50 | 56.18 | 51.28 | 53.47 |
| | $K_L$ (L $mg^{-1}$) | 0.0895 | 0.0699 | 0.0512 | 0.0417 |
| | $R^2$ | 0.9827 | 0.9867 | 0.9949 | 0.9926 |
| Freundlich | $K_F$ (mg $g^{-1}$) | 5.6712 | 4.7282 | 3.5656 | 3.1975 |
| | n (L $mg^{-1}$) | 2.261 | 2.085 | 1.950 | 1.850 |
| | $R^2$ | 0.9641 | 0.9765 | 0.9601 | 0.9580 |

**Table 2.** Comparison of the maximum adsorption capacity of various adsorbents.

| Adsorbent | Maximum adsorption capacity, $Q_m$ (mg $g^{-1}$) | | | | References |
|---|---|---|---|---|---|
| | $Pb^{2+}$ | $Cu^{2+}$ | $Zn^{2+}$ | $Cd^{2+}$ | |
| AO-ABS | 56.50 | 56.18 | 51.28 | 53.47 | present work |
| The commercial activated carbon (ST1000) | 43.00 | - | - | - | 34 |
| $Fe_3O_4$@3-aminopropyl triethoxysilane@Acrylic acid-co-Crotonic acid | 166.1 | 126.9 | 43.4 | 29.6 | 16 |
| Cassava tuber bark waste | - | - | 83.3 | 26.3 | 35 |
| Sugar beet pulp | 73.70 | 21.30 | 17.70 | 24.30 | 36 |
| Carrot residues | - | 45.09 | 29.61 | - | 37 |
| Peanut husk | - | 7.67 | - | - | 38 |
| Crosslinked chitosan with epichlorohydrin | 34.10 | 35.5 | 10.20 | - | 39 |
| Amidoximated Polyacrylo nitrile/Organo bentonite Composite | - | 77.43 | 65.40 | 52.61 | 22 |

**Table 3.** Kinetic models and their statistical parameters at 303K and at pH 6.0.

| Kinetic model | Parameters | Metal ions | | | |
|---|---|---|---|---|---|
| | | $Pb^{2+}$ | $Cu^{2+}$ | $Zn^{2+}$ | $Cd^{2+}$ |
| Pseudo-first-order | $K_1$ ($min^{-1}$) | 0.0131 | 0.0207 | 0.0184 | 0.0168 |
| | $Q_{e,cal}$ (mg $g^{-1}$) | 18.369 | 23.713 | 20.965 | 21.498 |
| | $R^2$ | 0.9824 | 0.9327 | 0.9257 | 0.9000 |
| Pseudo-second-order | $K_2$ (g $mg^{-1}$ $min^{-1}$) | 0.0011 | 0.0009 | 0.0008 | 0.0006 |
| | $Q_{e,\ cal.}$ (mg $g^{-1}$) | 27.932 | 28.089 | 28.169 | 28.328 |
| | $Q_{e,\ exp.}$ (mg $g^{-1}$) | 26.285 | 24.090 | 23.033 | 22.899 |
| | $R^2$ | 0.9975 | 0.9938 | 0.9918 | 0.9870 |

**Table 4.** Thermodynamics parameters for adsorption of the tested metal ions on AO-ABS.

| | $\Delta H(kJ\ mol^{-1})$ | $\Delta S(JK^{-1}\ mol^{-1})$ | $-\Delta G(KJ\ mol^{-1})$ | | | | |
|---|---|---|---|---|---|---|---|
| | | | 293 K | 303 K | 313 K | 323 K | 333 K |
| $Pb^{2+}$ | 36.383 | 128.601 | 37.643 | 38.929 | 40.215 | 41.501 | 42.787 |
| $Cu^{2+}$ | 24.027 | 85.251 | 24.954 | 25.807 | 26.659 | 27.512 | 28.364 |
| $Zn^{2+}$ | 30.812 | 104.931 | 30.714 | 31.763 | 32.812 | 33.861 | 34.912 |
| $Cd^{2+}$ | 22.215 | 74.671 | 21.856 | 22.603 | 23.349 | 24.096 | 24.843 |

Temperature = 293-333 K, $C_0$ = 100 mg $L^{-1}$, adsorbent dosage = 100 mg/25 mL, pH 6.0, immersion time = 120 min.

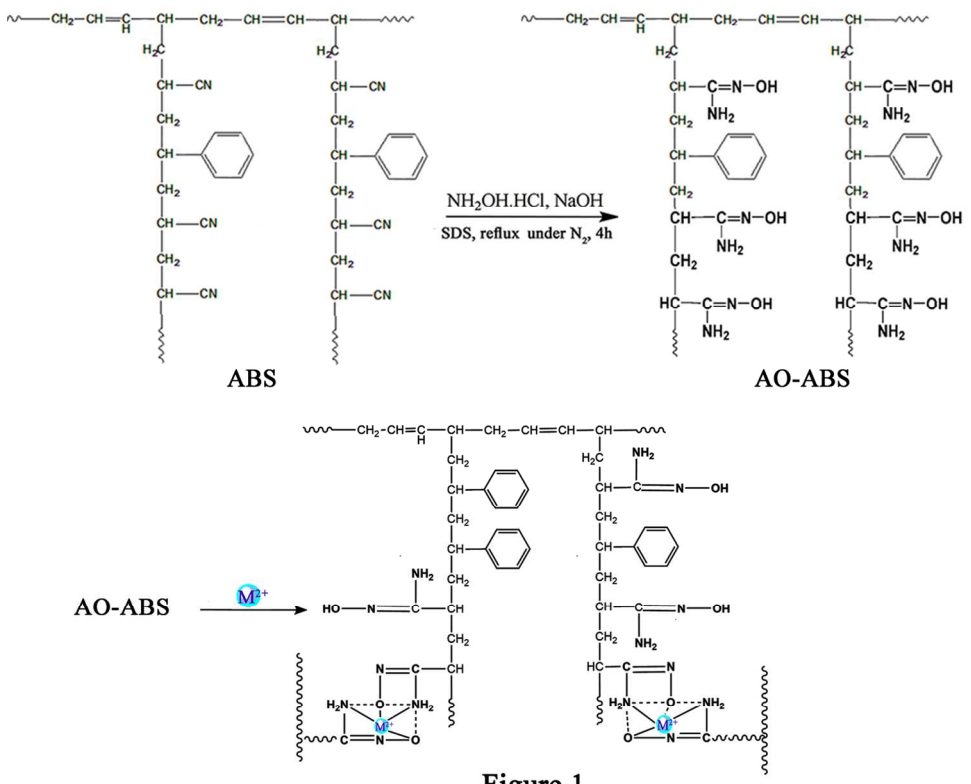


Figure 1

Figure 1. Conversion of ABS to AO-ABS; mixture of purified ABS waste powder, NH2OH.HCL/NaOH, and SDS in distilled water was refluxed 4 h under N2 atmosphere.
136x108mm (300 x 300 DPI)

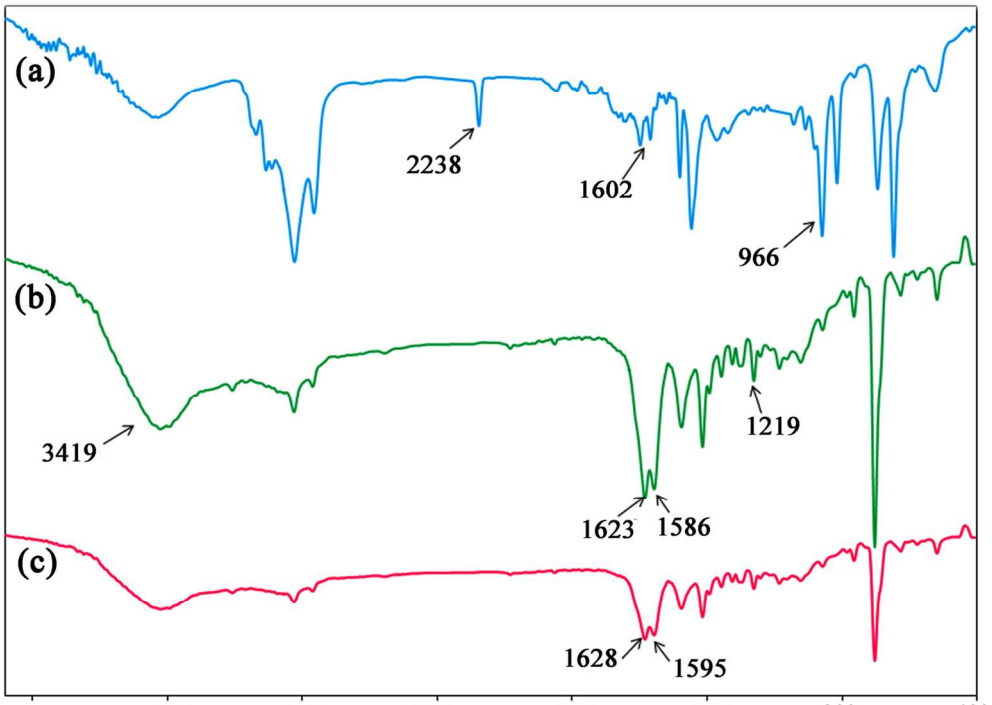


Figure 2. FT-IR spectra of ABS (a), AO-ABS (b), and metal-loaded AO-ABS (c)
67x54mm (600 x 600 DPI)

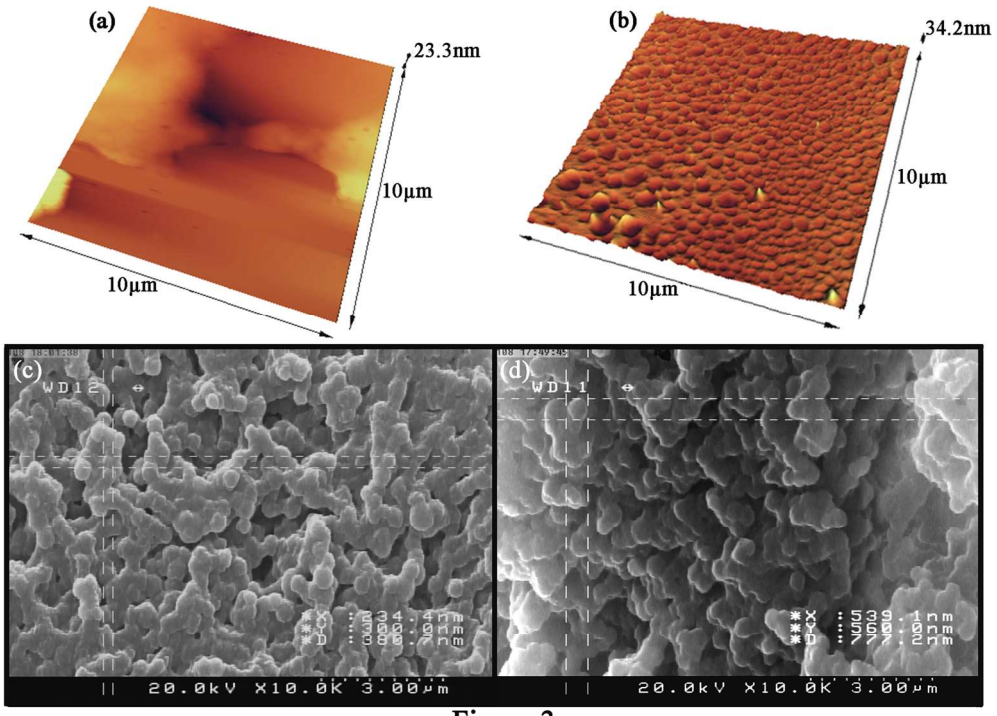


Figure 3

Figure 3. AFM images of AO-ABS before (a) and after (b) Pb2+ ion adsorption, and SEM images of AO-ABS before (c) and after (d) Pb2+ ion adsorption (Temperature = 303 K, C0 = 100 mg L−1, adsorbent dosage = 100 mg/25 mL, pH 6.0, immersion time = 120 min)
171x127mm (300 x 300 DPI)

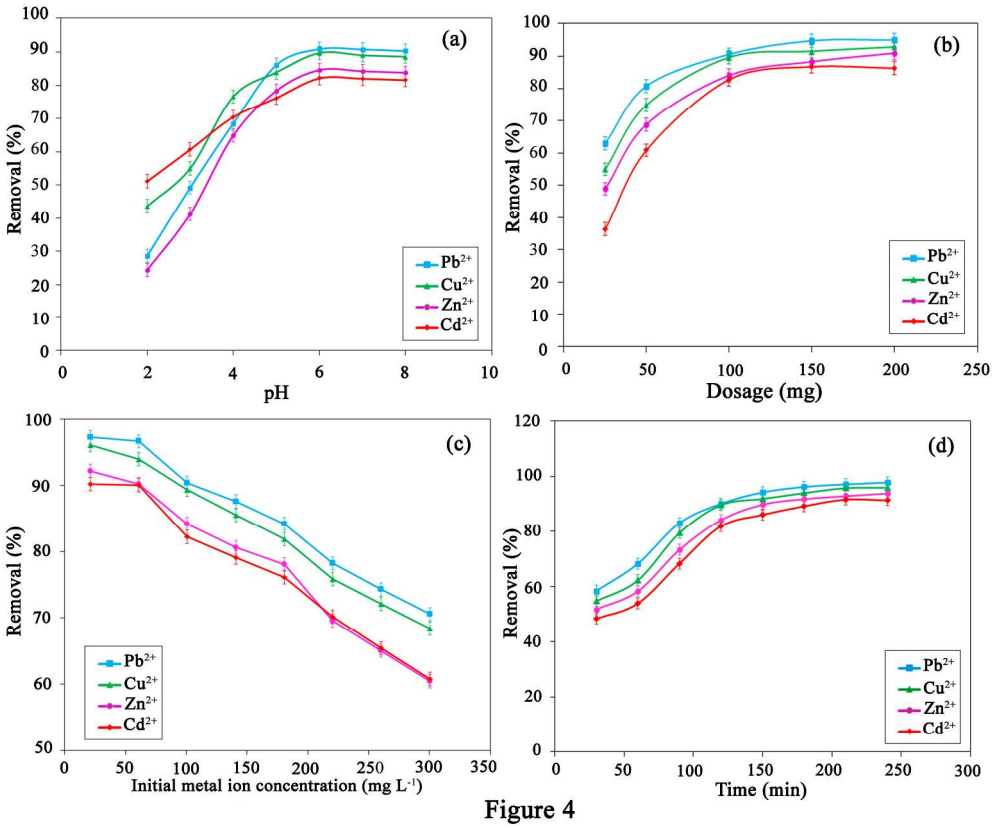


Figure 4

Figure 4. The effect of solution pH (2.0-8.0) (a), adsorbent dosage (25-200 mg/25 mL) (b), initial metal ion concentration (C0 = 20-300 mg L−1) (c) and immersion time (30-240 min) (d) on the removal efficiency of the tested metal ions. (Constant conditions: Temperature = 303 K, C0 = 100 mg L−1, adsorbent dosage = 100 mg/25 mL, pH 6.0, immersion time = 120 min, with varying the initial level of related factor).
142x118mm (600 x 600 DPI)

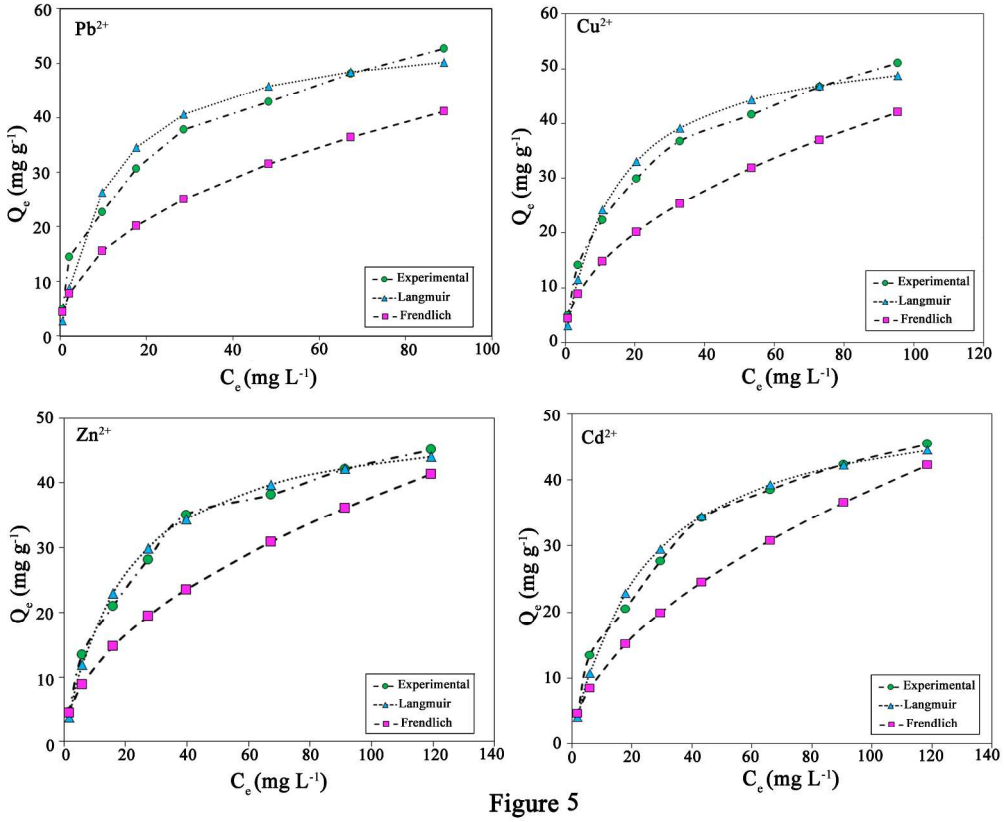


Figure 5

Figure 5. The adsorption isotherms of the tested metal ions on AO-ABS. (C0= 20-300 mg L-1, adsorbent dosage = 100 mg/25 mL, pH 6.0, temperature = 303 K, immersion time = 120 min).
143x121mm (600 x 600 DPI)

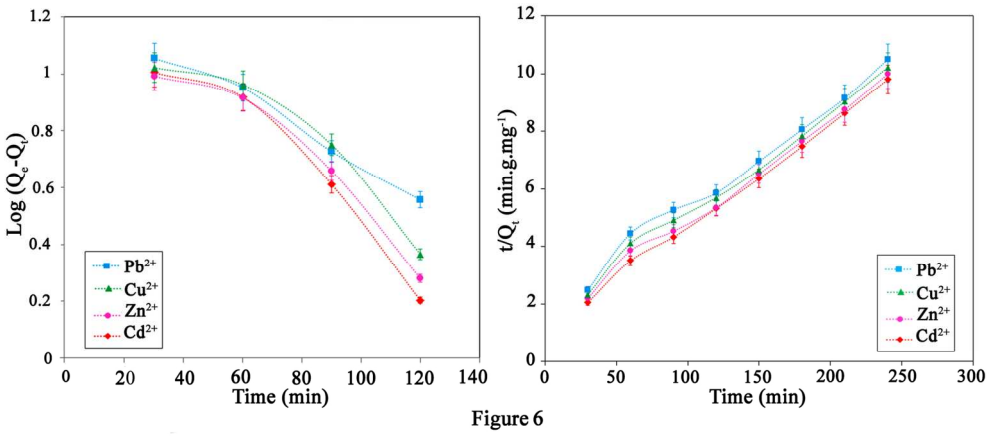


Figure 6

Figure 6. Kinetic models for the adsorption of the tested metal ions: (a) pseudo-first-order, (b) pseudo-second-order. (Temperature = 303 K, C0 = 100 mg L−1, adsorbent dosage = 100 mg/25 mL, pH 6.0, immersion time = 30-240 min).
74x32mm (600 x 600 DPI)

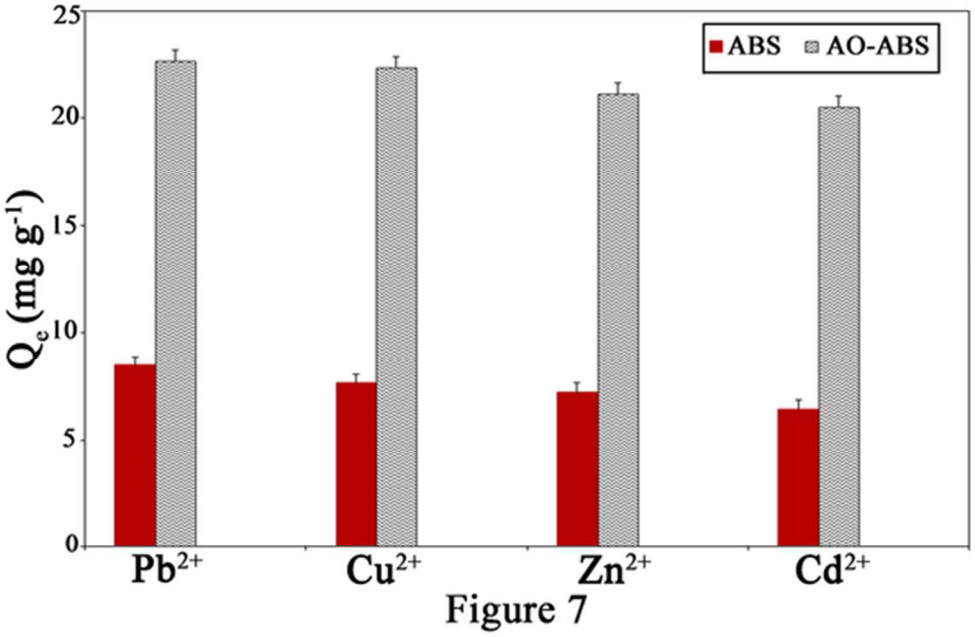


Figure 7. Comparison of the equilibrium adsorption capacity (Qe) of the tested metal ions on the untreated ABS and AO-ABS; (Temperature = 303 K, C0 = 100 mg L−1, adsorbent dosage = 100 mg/25 mL, pH 6.0, immersion time = 120 min).
51x33mm (300 x 300 DPI)

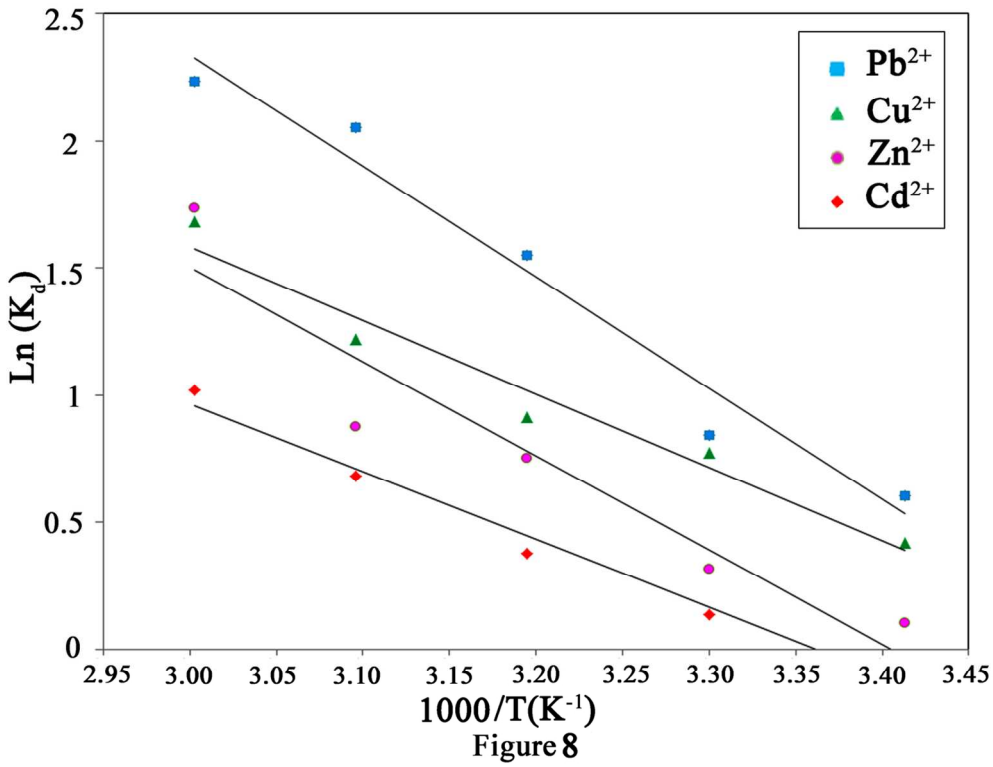


Figure 8. Van't Hoff plots of the tested metal ions adsorption (Temperature = 293-333 K, C0 = 100 mg L-1, adsorbent dosage = 100 mg /25 mL, pH 6.0, immersion time = 120 min).
61x46mm (600 x 600 DPI)

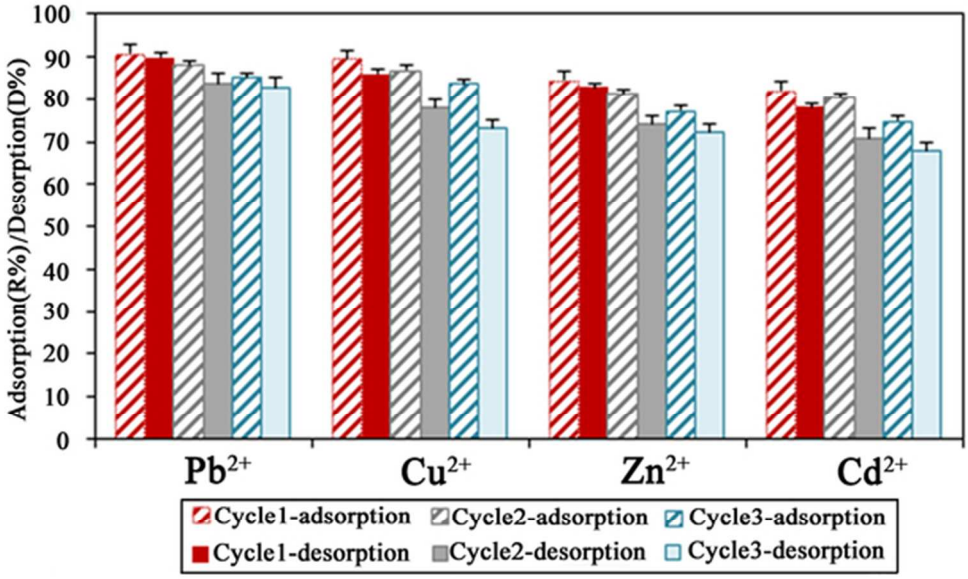


Figure 9

Figure 9. Adsorption/desorption percentages of the tested metal ions during 3 cycles. Desorption was carried out in 25 mL solution of HCl (0.1 M) and stirred for 1 h at 303 K.
53x34mm (300 x 300 DPI)

# Structural modification of Acrylonitrile–Butadiene–Styrene waste as an efficient nanoadsorbent for removal of metal ions from water: Isotherm, kinetic and thermodynamic study

**Arameh Masoumi, Khadijeh Hemati, Mousa Ghaemy***

Polymer Chemistry Research Laboratory, Chemistry Faculty, University of Mazandaran, Babolsar, Iran.

* Corresponding author: ghaemy@umz.ac.ir (Mousa Ghaemy) Tel/Fax.: +98-11-35342353

An environmentally benign approach for the structural modification of ABS waste and its use for the removal of heavy metal ions from aqueous solutions have been described using kinetics and isotherms studies.